IMA Fungus

IMA Genome - F15

Draft genome assembly of *Fusarium pilosicola, Meredithiella fracta, Niebla homalea, Pyrenophora teres* hybrid WAC10721, and *Teratosphaeria viscida*

Tuan Anh Duong[1], Janneke Aylward[1,2], Claudio Gennaro Ametrano[3], Barsha Poudel[4], Quentin Carlo Santana[1], Pieter Markus Wilken[1], Anke Martin[4], Kiruba Shankari Arun-Chinnappa[4,6], Lieschen de Vos[1], Isabel DiStefano[3], Felix Grewe[3] , Sabine Huhndorf[3], Helge Thorsten Lumbsch[3], Jostina Raesetsa Rakoma[1], Barsha Poudel[4], Emma Theodora Steenkamp[1], Yukun Sun[3] , Magriet A. van der Nest[1,5], Michael John Wingfield[1], Neriman Yilmaz[1] and Brenda Diana Wingfield[1*]

IMA GENOME-F 15A

Draft genome assembly of *Fusarium pilosicola*

Introduction

The *Fusarium fujikuroi* species complex (FFSC) is a diverse group of fungi with diverse ecologies that range from inhabiting soil to causing disease on a variety of plants (Kvas et al. 2009; Yilmaz et al. 2021). Members of this genus are also known for producing mycotoxins that are harmful to both human and animal health (Summerell 2019). Due to their economic importance, over 119 genome assemblies for species in the FFSC have been submitted to publicly available databases (https://ncbi.nlm.nih.gov), with the majority belonging to plant pathogens.

Fusarium pilosicola is a recently described FFSC taxon (O'Donnell et al. 2000; Yilmaz et al. 2021). The species was originally isolated in the USA from *Bidens pilosa*, commonly known as black-jack or cobblers pegs. Within the FFSC, *F. pilosicola* represents a sister clade to the economically important *Pinus* pathogen, *Fusarium circinatum* (O'Donnell et al. 2000; Yilmaz et al. 2021). *Fusarium pilosicola* shares morphological characteristics with *F. circinatum* and the closely related maize pathogen, *F.*

subglutinans, but differ from them by being unable to produce the typical purple pigment in culture (Yilmaz et al. 2021). Other than the traits included in typical descriptions of *Fusarium* species, not much is known about *F. pilosicola*. The genome sequence of this species therefore provides an important resource to investigate its genetics, overall biology and evolutionary history.

Sequenced strain

USA: *Florida*: Fort Pierce, 27.4467° N; 80.3256° W, isolated from *Bidens pilosa* (NRRL 29124, CMWF 1183, PREM 63216-dried culture) (Yilmaz et al. 2021).

Nucleotide sequence accession number

This Whole Genome Shotgun project has been deposited at DDBJ/ENA/GenBank under the accession JAGQDI000000000. The version described in this paper is version JAGQDI010000000.

Materials and methods

Fusarium pilosicola was grown on half strength potato dextrose agar (BD Difco™) at 25 °C for 7 days after which genomic DNA was extracted as previously described (Möller et al. 1992). The DNA was then subjected to sequencing on the MinION sequencer (Oxford Nanopore Technologies) using a MinION flow cell (R10.3). The raw MinION data (coverage 178) was assembled into scaffolds using the Flye assembler (version 2.8.1) (Kolmogorov et al. 2019). The draft assembly was then subjected to

*Correspondence: brenda.wingfield@fabi.up.ac.za
[1] Department of Biochemistry, Genetics and Microbiology, Forestry and Agricultural Biotechnology Institute (FABI), University of Pretoria, Private Bag X20, Hatfield 0028, South Africa
Full list of author information is available at the end of the article

Duong *et al. IMA Fungus*   (2021) 12:30
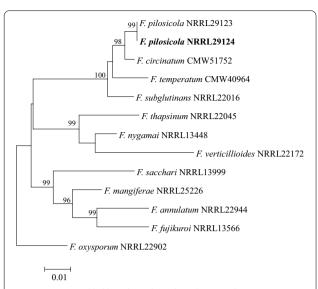
Page 2 of 17

Fig. 1 Maximum likelihood tree based on the partial gene sequences of translation elongation factor 1-α and β-tubulin (Herron et al. 2015; Wingfield et al. 2015, 2018). Sequence alignments were assembled with MAFFT v 7.472 (Katoh et al. 2019). The program jModelTest v 2.1.10 (Darribo et al. 2012) was used to determine the best-fit substitution model (TIM2 + G substitution model) with gamma correction (Tavare 1986). A maximum likelihood (ML) phylogenetic analysis was performed using PhyML v 3.1 (Guindon et al. 2010). Values at branch nodes are the bootstrapping confidence values with those ≥ 85% shown. The *F. pilosicola* isolate sequenced in this study was indicated in bold

two sequential rounds of error correction using RACON (version 1.4.17) (Vaser et al. 2017a, b). To confirm the identity of the sequenced isolate, we extracted relevant portions of the genes encoding translation elongation factor 1-α and β-tubulin, and used these in phylogenetic analyses (see the legend of Fig. 1 for detail).

Completeness of the genome assembly was evaluated with BUSCO (version 4.1.0) using Hypocreales_odb10 gene dataset (Seppey et al. 2019). Genome annotation was done with the MAKER pipeline (version 2.31.8) (Holt and Yandell 2011), which incorporated gene prediction tools AUGUSTUS (version 3.2.3) (Keller et al. 2011), GeneMark-ES (Ter-Hovhannisyan et al. 2008) and SNAP (Korf 2004). Gene model data from *F. circinatum* (Wingfield et al. 2012), *F. fujikuroi* (Wiemann et al. 2013), *F. verticillioides* and *F. graminearum* (Ma et al. 2010), as well as *F. mangiferae* and *F. proliferatum* (Niehaus et al. 2017), were included as additional evidence.

Results and discussion

The genome sequence of *F. pilosicola* (NRRL 29124) consisted of 95 scaffolds with a total genome size of 47 881 020 bp, an N50 value of 3 565 285 bp and G + C content

of 47.04%. Phylogenetic analysis based on sequences extracted from this assembly, confirmed the taxonomic identity of the sequenced strain as *F. pilosicola* (Fig. 1). BUSCO analysis showed that the assembly was 97.5% complete, containing 97.3% complete and single-copy BUSCOs, 0.2% complete and duplicated BUSCOs; 2.2% fragmented BUSCOs, 0.3% missing BUSCOs (n = 4494). A total of 14 928 gene models were predicted using the MAKER annotation pipeline.

Sequence comparisons to the genomes of *F. circinatum* (NCBI accession: GCA_000497325.3) (Wingfield et al. 2018) and *F. temperatum* (NCBI accession: GCA_001513835.1) (Wingfield et al. 2015) indicated that scaffolds corresponding to all twelve of the known chromosomes for species in the FFSC are present in the *F. pilosicola* assembly. These comparisons also showed that the overall size and coding content of the *F. pilosicola* genome corresponded with those reported for other members of the so-called American Clade of the FFSC (O'Donnell et al. 1998). At 47.95 Mbp, the *F. pilosicola* genome is 2.45 Mbp larger in size than the 45.5 Mbp *F. temperatum* genome and 4.02 Mbp larger than the 43.93 Mbp *F. circinatum* genome. Despite these size differences, however, approximately 600 fewer genes were predicted for the *F. pilosicola* genome compared to those for *F. temperatum* and *F. circinatum*.

Fusarium pilosicola was isolated from *B. pilosa* in Florida which (O'Donnell et al. 2000) and its closest known relative is *F. circinatum* (Yilmaz et al. 2021), which is believed to have originated in Mexico and Central America (O'Donnell et al. 1998; Wikler and Gordon 2000). It was hypothesised that *F. pilosicola* moved with its noxious weed host when it expanded its range from the neotropics. Such an overlap in the geographic distribution these fungi's plant hosts suggest their centres of origin likely also overlap, which would be consistent with their recent shared ancestry (Yilmaz et al. 2021). Availability of the genome of *F. pilosicola* will contribute to investigations into this phylogenetic relatedness.

Authors: **Quentin C. Santana***, **Lieschen De Vos, Neriman Yilmaz, Tuan A. Duong, Magriet A. van der Nest, Emma T. Steenkamp, Brenda D. Wingfield**
**Contact*: quentin.santana@fabi.up.ac.za

IMA GENOME-F 15B

Complete genome assembly of *Meredithiella fracta*

Introduction

Members of the fungal family *Ceratocystidaceae* have a well-established association with insects. For many genera this relationship lacks specificity (De Beer et al. 2014; Wingfield et al. 2013; Kirisits 2004), although some species form specific, mutualistic associations with ambrosial

Duong *et al. IMA Fungus* (2021) 12:30

Page 3 of 17

beetles (Mayers et al. 2020, 2015, 2018; Harrington et al. 2014). These fungi are carried in relatively large, specialized body cavities known as mycangia (Six 2003; Batra 1963). Adult beetles will inoculate the fungal symbiont from their mycangia into the sapwood of dead or dying trees where both the larvae and adult beetles will feed on the fungal growth (Harrington 2005). *Ceratocystidaceae* species which are ambrosial symbionts were historically grouped in the genus *Ambrosiella* (Harrington et al. 2010), although this group was plagued by a lack of monophyly (Massoumi Alamouti et al. 2009; Mayers et al. 2018). Subsequent studies have recognized four bark-beetle associated genera additional to *Ambrosiella*. These are the genera *Phialophoropsis* associated with beetles from the tribe *Xyloterini* (Mayers et al. 2015), *Toshionella* as symbionts of Asian *Scolytoplatypus* beetles (Mayers et al. 2020), *Wolfgangiella* as ambrosial fungi of African *Scolytoplatypus* species (Mayers et al. 2020) and *Meredithiella* for symbionts of the beetle genus *Corthylus* (Mayers et al. 2018).

Currently three species are recognized in the genus *Meredithiella*, although some cryptic taxa remain unresolved (Mayers et al. 2015, 2018). *Meredithiella norrisii* is the type species of the genus and was first described from galleries of *Corthylus punctatissimus* in the USA (Mayers et al. 2015). Subsequently, this fungus was also found in *C. columbianus*, also from the USA (Mayers et al. 2018). *Meredithiella guianensis* was isolated from the galleries and mycangia of *Corthylus crassus* from French Guiana, and is morphologically very similar to *M. norrisii* with size differences in the aleurioconidia being a distinguishing characteristic (Mayers et al. 2018). The third species, *M. fracta*, was isolated from the mycangium of *Corthylus papulans* beetles from the USA and Honduras (Mayers et al. 2018).

In this study a chromosome-level assembly of the exholotype of *M. fracta* is presented. This genome was produced using long-read nanopore sequencing together with short-read Illumina sequences. This genome is the first for any species in the genera *Phialophoropsis*, *Toshionella*, *Wolfgangiella*, or *Meredithiella*, and complements the two *Ambrosiella* genomes currently publicly available (Vanderpool et al. 2017; Wilken et al. 2020).

Sequenced strain
USA: *Florida*: Alachua County, Gainesville, dried culture isolated from mycangium of *Corthylus papulans,* 23 Feb 2016, *C. Bateman* (BPI 910531—holotype, dried culture; CBS 142645—ex-holotype culture).

Nucleotide sequence accession number
This Whole Genome Shotgun project has been deposited at DDBJ/ENA/GenBank under the accession JAGXCV000000000. The version described in this paper is version JAGXCV010000000.

Materials and methods
The ex-holotype isolate of *Meredithiella fracta* (CBS142645) was obtained from the culture collection of the Westerdijk Fungal Biodiversity Institute, Utrecht, The Netherlands. The culture was grown on YM (0.5% yeast extract, 2% malt extract, Biolab, South Africa) at 25 °C for 5 days. The QIAGEN Genomic-tips (Qiagen, Germany) was used to extract DNA from the culture using the protocol for plants and filamentous fungi, which was used to generate Nanopore sequencing reads on the MinION sequencing device (Oxford Nanopore Technologies, Inc., Oxford, UK). A sequencing library was prepared using the Genomic DNA by Ligation kit (SQK-LSK109) and was loaded on a MinION flow cell (R10.3) for a 48 h sequencing run. Base calling was conducted using the ONT Guppy basecalling software v 4.0.14. The resulting Nanopore reads were loaded onto the Galaxy bioinformatics platform (https://usegalaxy.eu); (Afgan et al. 2016), and used to generate a draft genome assembly with the Canu v 2.1.1 assembler (Koren et al. 2017).

Illumina sequencing data were generated at the Agricultural Research Council Biotechnology Platform (ARC-BTP; Pretoria, South Africa). The *M. fracta* DNA was used to prepare a pair-end library with a median insert size of 550 bp. An Illumina HiSeq 2500 instrument (Illumina, San Diego, USA) was used to generate paired-end reads of 150 bp. The raw reads were uploaded to Galaxy (Afgan et al. 2016) as separate libraries. Any adaptor sequences and low-quality reads were trimmed from the read libraries using a combination of Trimmomatic v. 0.38.1 (Bolger et al. 2014), Cutadapt (Martin 2011) and Trim Galore! v. 0.4.3.1 (a wrapper of the Cutadapt program). The trimmed illumina paired-end data were mapped to the Nanopore genome assembly using BWA-MEM (Li and Durbin 2009), and the resulting BAM file was used to polish the Nanopore assembly using Pilon v. 1.20 (Walker et al. 2014a, b).

The number of protein coding genes present in the genome was estimated in Galaxy using the AUGUSTUS de novo prediction software v. 3.3.3 with *Fusarium graminearum* gene models (Keller et al. 2011; Stanke et al. 2006a, b). Genome statistics including genome length, GC content, N50 and L50 values were calculated using QUAST v. 5.0.2 (Mikheenko et al. 2018), while completeness against the Fungi_odb10 and Ascomycota_odb10 datasets were determined using the Benchmarking Universal Single Copy Orthologs tool (BUSCO v. 5.0.0) (Simão et al. 2015) implemented using default parameters. To confirm the identity of the sequenced strain, the eukaryotic translation elongation factor 1 alpha (TEF1)

Duong *et al. IMA Fungus*   (2021) 12:30

Page 4 of 17

gene was extracted from the assembly of *M. fracta* using CLC Main Workbench v21.0.2 and used together with representative sequences from other Ceratocystidaceae species in a phylogenetic analysis. To do this, the one-click mode of the Phylogeny.fr online tool (Dereeper et al. 2010, 2008) that includes alignment via MUSCLE (Edgar 2004), Gblocks alignment refinement (Castresana 2000) and tree construction using PhyML (Guindon et al. 2010; Guindon and Gascuel 2003) was used. An approximate likelihood-ratio test was used to determine branch support (Anisimova and Gascuel 2006).

Results and discussion
The nuclear genome assembly of *M. fracta* had a length of 27,045,695 bp present in 11 scaffolds, of which 9 were 1.3 Mb or larger. The genome had a GC content of 46.64%, a N50 value of 3,970,047 bp and a L50 value of 3. The BUSCO analyses reported good completeness scores (89.2% for the 1706 ortholog Ascomycota dataset and 93.6% for the 758 ortholog Fungi dataset), with 1522 complete and 118 missing orthologs in the Ascomycota set and 710 complete and 26 missing orthologs in the Fungi dataset. AUGUSTUS de novo gene prediction using the *F. graminearum* gene models predicted 6296 protein coding genes, while phylogenetic analysis of the *TEF1* gene confirmed the identity of the isolate as *M. fracta* (Fig. 2).

The *M. fracta* genome has been assembled to a high level of completeness. Nine scaffolds are larger than 1 Mb, corresponding to the predicted number of chromosomes for the *Ceratocystis* species *C. fimbriata* and *C. manginecans* (Fourie et al. 2019). The two additional scaffolds that make up the *M. fracta* assembly are orders of magnitude smaller (~ 21 kb and ~ 31 kb), and likely represents unassembled fragments of the genome rather than accessory chromosomes. This is supported by the fact that none of the 6296 putative protein coding genes were predicted on either of these two chromosomes. An earlier comparative genomics study on *C. albifundus* also found that the genome contains no dispensable chromosomes, with accessory genomic components spread throughout the genome (Van der Nest et al. 2019).

Meredithiella fracta is the first of several genomes currently being sequenced for species of *Phialophoropsis*, *Toshionella*, *Wolfgangiella* and *Meredithiella* (Wilken et al. unpublished). These fungal lineages have only recently been delineated (Mayers et al. 2015, 2020), but have already impacted the study of ambrosial symbionts (Nel et al. 2020; Skelton et al. 2018; Vanderpool et al. 2017). The availability of full genome sequences for these and other Ceratocystidaceae ambrosial fungi (such as *Ambrosiella*; Vanderpool et al. 2017; Wilken et al. 2020) will add a genomic toolset for use in future studies. This includes genomes with a high level of accuracy (such as that of *A. cleistominuta* with a 98% BUSCO value; (Wilken et al. 2020) as well as assemblies with a high level of completeness (e.g. the genomes of *A. xylebori* (38 scaffolds; Vanderpool et al. 2017) and *M. fracta* (11 scaffolds; current study)). These could support a range of studies in future, including understanding the beetle-fungus symbiosis, comparative genomics of ambrosial fungi and developing tools for taxonomic studies on these fungal groups.

Authors: **P. Markus Wilken*, Jostina R. Rakoma, Tuan A. Duong, Brenda D. Wingfield**
*Contact: Markus.Wilken@fabi.up.ac.za

IMA GENOME-F 15C
Draft genome sequence of *Niebla homalea* (*Ramalinaceae*)
Introduction

Ramalinaceae is the fourth-largest family of lichenized ascomycetes with 42 genera and 913 currently accepted species exhibiting considerable morphological variation (Kistenich et al. 2018), and with 42 species of fruticose lichens which are recognized in the genus *Niebla* (Spjut 1996). As the genus name suggests, species of this genus thrive in fog-dependent ecosystems; the genus *Niebla* is indeed endemic to the New World coastal fog deserts (Sérusiaux et al. 2010). It occurs in two geographically disjunct coastal fog deserts along the Pacific coast of North and South America, the Baja California Peninsula and the Atacama Desert of northern Chile (Rundel 1978a). In this peculiar environment, the combined effects of frequent conditions of high atmospheric humidity and strong sea breezes restricts vascular plant vegetation and allows a remarkable lichen community to develop (Rundel et al. 1972) which express a relatively high levels of endemism at both the species and genus levels (Rundel 1978a, b; Rundel et al. 1991).

Niebla homalea, previously named *Desmazieria homalea* (Montagne 1852; Rundel 1978b), is the type species of the genus *Niebla*, and one of the most representative species of coastal deserts (Rundel et al. 1972). It occurs in association with other *Niebla* species and other species adapted to this environment (e.g. *Vermilacinia*, *Roccella*), which are able to efficiently exploit fog water by means of their growth form (Stanton and Horn 2013) and poikilohydric life-style (Green et al. 2011).

Within fruticose *Ramalinaceae* lichens, species are well resolved in the genera *Namibialina* and *Ramalina*. Also, the sister clade, *Vermilacinia,* is relatively well resolved, supporting the current species delimitation (Spjut et al. 2020). Species delimitation in *Niebla* is less straightforward; secondary metabolite variation generally coincides with major clades from molecular phylogenegetics, however, these clades often include samples from different

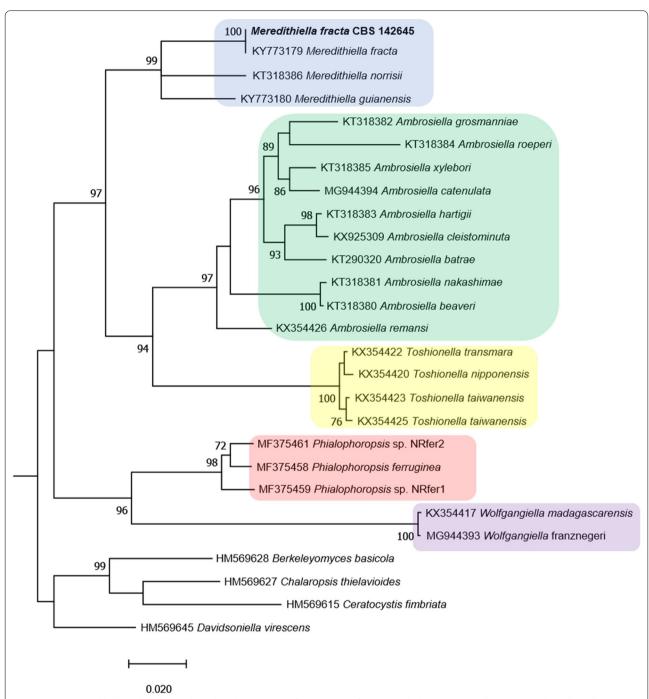Duong *et al. IMA Fungus*   (2021) 12:30

Page 5 of 17

Fig. 2 A maximum-likelihood phylogeny based on the *TEF1* gene from species of *Meredithiella* (blue), *Ambrosiella* (green), *Toshionella* (yellow), *Phialophoropsis* (red) and *Wolfgangiella* (purple). This analysis confirms the identity of the genome assembly presented here (shown in bold) as *Meredithiella fracta*. *Berkeleyomyces basicola*, *Chalaropsis thielavioides*, *Ceratocystis fimbriata* and *Davidsoniella virescens* were used as outgroups, and the results for the approximate likelihood ratio test for branch support are shown as percentages

morphologically described species (Spjut et al. 2020). A recent attempt to use next-generation sequencing, such as RADseq, provided crucial information about the diversification history of *Niebla*, however, it remained challenging to completely resolve this group (Jorna et al. in review).

We sequenced the first draft genome of the lichenized fungus *Niebla homalea.* The specimen for the mycobiont

Duong *et al. IMA Fungus* (2021) 12:30

Page 6 of 17

isolation was collected at the Shell Beach in the Sonoma Coast State Park, California. *Niebla homalea* is morphologically characterized by a fruticose thallus that is divided into many large branches and often with numerous smaller branches. The cortex is glossy, yellowish to olivaceous green, and often has black patches (Spjut 1996).

Our genome sequence of *N. homalea* will serve as a reference for future phylogenetic and comparative genomics studies involving members of *Ramalinaceae*. The genome sequence may aid in obtaining a better understanding of genomic factors that make the *Niebla* genus endemic to coastal fog deserts, an environment with limited supply of liquid water and characterized by harsh abiotic conditions. Furthermore, as the lichen communities of coastal deserts will face further challenges in the near future, such as those determined by climate change and the increase of land consumption in coastal areas, the genome sequence of *N. homalea* will also be of great value in a conservation genomics perspective.

Sequenced strain
USA: *California*: Sonoma Coast State Park; 38.420805, −123.111199; Shell Beach, collected on a large rock, 25 Jul/2018, *S.M. Huhndorf and T.J. Widhelm* (F C0395311F, dried specimen). Lichen-fungus culture: *S.M. Huhndorf* Field Museum culture lab strain fmnib47.

Nucleotide sequence accession number
The draft whole-genome sequence of the lichen-fungus *Niebla homalea* has been deposited at DDBJ/EMBL/Genbank under the accession number JAHGAU000000000. The version described in this paper is version JAHGAU010000000. Accession for SRA data: PRJNA707213.

Materials and methods
Axenic cultures were produced from lichen spores and grown on media until the individual cultures reached sufficient sizes for DNA extraction. A high-molecular weight (HMW) DNA extraction of the lichen-fungal culture was performed following the protocol published by Benjamin Schwessinger (https://doi.org/10. 17504/protocols.io.exmbfk6) with modifications, as for the lichen-fungus genome sequencing of *Physcia stellaris* (Wilken et al. 2020). About 0.6 g of dried fungal culture material was flash frozen with liquid nitrogen and ground with a ceramic mortar and pestle, then allowed to reach room temperature. The ground material was incubated with 500 µL lysis buffer and 20 µL proteinase K at 64 °C up to 4 h, then cooled on ice for 5 min. To the cool mixture 100 µL KAc 5 M was added and incubated

for 5 min on ice, then centrifuged at max speed at 4 °C for 10 min. The supernatant was added to 500 µL phenol:chloroform:isoamyl alcohol (25:24:1) and centrifuged at max speed at 4 °C for 10 min. The supernatant was added to 500 µL isopropanol and cooled at −80 °C for 1 h. The isolated HMW DNA was precipitated at max speed at 4 °C for 30 min, washed twice with 1 mL 70% ethanol, and eluted in 50 µL TE buffer.

Isolated HMW DNA was converted into Nanopore libraries with the NBD103 and 1D library kit SQK-LSK 109 (Oxford Nanopore Technologies Inc., UK). The libraries were sequenced on a SpotON R9.4.1 FLO-MIN106 flowcell for 48 h, using a GridIONx5 sequencer. The raw sequencing data was basecalled with guppy v. 3.0.3 (https://pypi.org/project/guppy3/3.0.3/), then adaptor trimmed with Porechops v. 0.2.3 (https://github.com/rrwick/Porechop). In addition, the same DNA sample was converted into Illumina sequencing libraries with the Hyper Library construction kit from Kapa Biosystems (Roche GmbH, Germany) and paired-end sequenced for 251 cycles on a MiSeq Illumina sequencer using the MiSeq 600-cycle sequencing kit v. 3 (Illumina Inc., Ca, US). All raw Illumina reads were trimmed with Trimmomatic v. 0.33 (Bolger et al. 2014), setting a quality threshold of 10 (LEADING:10 TRAILING:10). Library construction and sequencing were done at the DNA services facility at the University of Illinois at Urbana-Champaign.

The Nanopore reads were assembled into contigs using Flye v. 2.8-b1674 (Kolmogorov et al. 2019, b) or Canu (Koren et al. 2017). These assembled contigs were further aligned twice with Nanopore raw reads for error correction and scaffolding by using bwa v. 0.7.17-r1188 (Li and Durbin 2010) within the Racon v. 1.4.13 pipeline (Vaser et al. 2017a, b). The resulting consensus contigs were further polished twice with the trimmed Illumina reads by using bwa within the Pilon v. 1.23 pipeline (Walker et al. 2014a, b). The assembly quality was benchmarked using QUAST v. 5.0.2 (Gurevich et al. 2013). The genome completeness was estimated by BUSCO 4.0.6 (Simão et al. 2015) using the ortholog data set for Ascomycota (1706 genes).

The polished genome assembly was pre-annotated with MAKER 3.01.03 (Cantarel et al. 2008) using *Aspergillus nidulans* as the gene model species in AUGUSTUS v. 3.4.0 (Stanke et al. 2006a, b). The identified genes were then functionally annotated by using (1) InterProScan v. 5.47-82.0 (Jones et al. 2014), (2) UniProtKB Swiss-Prot, and (3) TrEMBL databases (March 2020). The *Niebla* genes were also searched for homologs against the prior annotation of the lichen-fungus *Physcia stellaris* (Wilken et al. 2020) using tblastn (BLAST v. 2.2.31) with an E-value cutoff of 1e−30, which served as a fourth

Duong *et al. IMA Fungus*   (2021) 12:30

Page 7 of 17

dataset for gene functionality. For the final functional annotation best gene annotations were manually selecting from these four datasets. Secondary metabolites were predicted using antiSMASH v. 6.0.0alpha1-820a4b7 (Blin et al. 2019).

The *N. homalea* genome identity was determined with phylogenetic analyses of the internal transcribed spacer (ITS) barcoding marker sequence, together with other five loci commonly used in fungal phylogenies: ribosomal large subununit (LSU), glyceraldehyde-3-phosphate dehydrogenase (GDP), RNA polymerase II largest and second largest subunits (RPB1, RPB2) and translation elongation factor 1-alpha (tefa). These loci were identified with a BLASTn search using *Niebla* sequences available on NCBI as queries. The ITS region (ITS1, 5.8S, and ITS2) and the other loci extracted from the *Niebla* assembly were aligned with 101 samples from 27 *Niebla* species (Spjut et al. 2020) using MAFFT v. 7.475 (Katoh and Standley 2013). The resulting alignments were manually curated to remove ambiguously aligned nucleotide positions. Bayesian phylogenetic analysis was conducted running BEAST v. 2.6.1 (Bouckaert et al., 2014). Tree topology was linked across the six loci while clock and site model were left unlinked. The substitution model was set to GTR+G for each locus partition with gamma shape estimated and five rate categories; substitution rates were estimated. Clock model and priors were set to default values. Sequences from *Vermilacinia procera* and *Ramalina farinacea* were added to the dataset as outgroup but without setting them as an outgroup prior. The Maximum Clade Credibility (MCC) tree was generated from 45,000 trees sampled from two BEAST runs of $5*10^8$ generations after 10% of the sampled trees was discarded as burn-in; runs convergence was inspected in Tracer v. 1.7 (Rambaut et al. 2018), effective sample size values were greater than 200 for each of the sampled parameters. The node support of the resulting phylogenetic tree was evaluated as posterior probabilities in FigTree v1.4.2 (http://tree.bio.ed.ac.uk/software/figtree).

Results and discussion

The genome of the lichen-fungal culture *Niebla homalea* using Fly assembled into 52 contigs with a total length of 50.6 Mb. The final assembly contained only contigs larger than 25 Kb, with the largest being 3.158 Mb (Table 1). This assembly was used for further analyses since it outperformed the Canu assembly (111 contigs, N50 = 973 Kb). All contigs resulted in a N50 of 1.266 Mb with a GC content of 37.96%. The mean assembly coverage was 22× of Nanopore sequences and 21× of Illumina sequences. BUSCO analysis estimated a genome completeness of 96%, with only 0.2% duplicated genes and 4%

fragmented or missing genes out of the 1706 Ascomycota single copy orthologs searched. Augustus gene modeling predicted a total of 9355 genes, resulting in an average gene density of 185 genes/Mb. These genes were interrupted by 17,778 introns; hence each gene contained on average 1.9 introns.

The genome contained 44 gene clusters associated to secondary metabolite biosynthesis. Among them were identified 30 Type I and a single Type III polyketides synthetases (PKSs), 7 non-ribosomal peptide synthetases (NRPSs), and 4 NRPS-like fragments. In addition, antiSMASH identified 5 terpene gene clusters.

The draft genome is larger than the average for the Lecanoromycetes, the class to which *N. homalea* belongs, draft genomes sequenced to date (37.1 Mb; Apr 2021). In particular the *N. homalea* assembly is noticeably larger than the two other lichens belonging to the Ramalinaceae family whose draft genomes are publicly available: *Ramalina peruviana* (26.2 Mb) and *Ramalina intermedia* (27 Mb) (Wang et al. 2018). Moreover, the *N. homalea* assembly differs from most of the other sequenced Lecanoromycetes genomes in its GC content (37.96%), which is lower than the average of the class (46%). The difference is even more striking when considering the closely related *Ramalina* genomes, which have an average GC content of 51%. However, these differences could have

Table 1 Genome overview

Assembly	Flye	Canu
Assembly size (Mb)	50.57	51.63
Contigs	52	111
Contig N50 (Kb)	1267	972
Mean Coverage by Nanopore (fold)	22	22
Mean Coverage by Illumina (fold)	21	21
G + C content (%)	37.96	37.65
BUSCO completeness	C:96.0%[S:95.8%,D:0.2%],F:0.5%,M:3.5%	
Gene prediction		
Predicted gene models	9355	
Average gene length (bp)	1586.97	
Gene density (genes per Mb)	184.99	
Predicted introns	17 778	
Introns per gene	1.9	
Secondary metabolites		
Total SM clusters	44	
Type I polyketide synthetases (PKSs)	30	
Type III PKSs	1	
Nonribosomal peptide synthetases (NRPSs)	7	
NRPS-like fragments	4	
Terpene clusters	5	

Duong *et al. IMA Fungus* (2021) 12:30

Page 8 of 17

been magnified by the different sequencing methods used. All *Ramalina draft* genomes were assembled from Illumina libraries while *N. homalea* was assembled from both Illumina and Nanopore libraries, which are less afflicted by GC bias (Browne et al. 2020).

The *N. homalea* genome assembled into a high-quality draft genome. The contiguity of the genome is comparable to other hybrid assemblies of lichen-forming fungi assembled from a combination of short and long reads technologies, or recent genomes only assembled from high coverage of long reads, such as the *Letharia columbiana* draft genome (McKenzie et al. 2020). Similar results were only obtained by using extremely high coverage of Illumina short reads, such as in *Cladonia metacorallifera* (Park et al. 2014) or *Umbilicaria muehlenbergii* (Park et al. 2014) draft genomes. However, it is generally difficult to obtain chromosome level genome assemblies by only relying on short reads and whole genome shotgun sequencing, as highlighted by the lower contiguity of most *Lecanoromycetes* draft genomes assembled form short reads only (data not shown).

The lack of a class-level orthologs database for *Lecanoromycetes*, limited the BUSCO completeness analysis sensitivity, however the *N. homalea* assembly performed in line with expectation and showed a similar completeness to the best assemblies produced so far within the class. The maximum BUSCO completeness in *Lecanoromycetes* draft genomes to date is 97.8%, reached by the highly contiguous (7 scaffolds) *Umbilicaria muehlenbergii* genome, while most other the high-quality draft genomes were at 94–97% completeness (data not shown).

The phylogenetic relationships and the species delimitation within the genus *Niebla* proved to be difficult to resolve following an integrative taxonomy approach, and even using multi-locus inferences and a wide taxon sampling it remains problematic (Spjut et al. 2020). Inference solely based on the ITS region, indeed, lacked the phylogenetic signal needed to confirm the species identity of the here assembled genome with confidence, as it was characterized by a lack of statistical support with many branches forming polytomies, especially using a maximum likelihood approach (data not shown). The six loci Bayesian phylogeny provided improved resolution (Fig. 3), allowing the identification of the sequenced draft genome as belonging to the clade of *N. homalea.* The clade where the genome sample was placed in our phylogeny is highly supported, and it is consistent with the one identified by the original phylogeny (Spjut et al. 2020), however, as mentioned, within this clade are present different morphologically described species.

The availability of the *N. homalea* draft genome from this study will allow comparative genomic studies within *Ramalinaceae.* It will also add to the genomic database of lichenized fungi for future research of evolutionary biology, aiming at an improvement of our understanding of molecular trends that were shaped by the lichen symbiosis. Moreover, *N. homalea* being endemic to coastal fog deserts, its genome sequence could be used for comparative analyses with cosmopolitan lichenized fungi able to colonize similar environments, in order to understand if there is any genome adaptation peculiar to coastal deserts lichens.

Authors: **Claudio Ametrano*** **Yukun Sun, Isabel DiStefano, Sabine Huhndorf, H. Thorsten Lumbsch, and Felix Grewe**

**Contact*: Claudio Ametrano claudiog.ametrano@gmail.com

Table 1 *Niebla homalea* draft genome overview. BUSCO completeness reported as percentage of complete (C), single copy (S), duplicated (D), fragmented (F), missing (M) genes. Basic statistics reported for both Flye and Canu assemblies. Flye assembly was used for all the subsequent analyses.

IMA GENOME – F 15D

Short-read genome assembly and annotation of a field collected *Pyrenophora teres* f. *teres* x *P. teres* hybrid WAC10721

Introduction

Pyrenophora teres f. *teres* and *P. teres* f. *maculata* are the causal agents of the net blotches, which are major foliar diseases of barley worldwide and may cause complete yield losses under favourable conditions (Liu et al. 2011; Mathre 1982; McLean et al. 2009). These haploid fungi occur as two forms, *P. teres* f. *teres* and *P. teres* f. *maculata*, based on the formation of net and spot like symptoms on barley leaves, respectively. Both forms co-exist in the field and produce sexual sporing bodies on stubble, releasing ascospores which act as the primary source of inoculum. Sexual reproduction between the two forms of *P. teres* has been induced in the laboratory and some of these *P. teres* hybrids have shown reduced sensitivity to triazole fungicides and were highly virulent on some barley genotypes (Campbell and Crous 2003; Campbell et al. 1999, 2002; Jalli 2011; Poudel et al. 2018). Hybrids between *P. teres* f. *teres* and *P. teres* exist in nature and to date two hybrids have been identified in Australia (McLean et al. 2014, 2020). One of the field hybrids collected in Western Australia was found to be rapidly spreading clonally and had resistance to some Group 3 compounds of azole or demethylation inhibitors fungicides (Lopez-Ruiz et al. 2020). The evolution of such new pathotypes would provide additional challenges when deploying resistant barley varieties. Therefore, to shed light on the genetic architecture and diversity of this emerging pathogen, we undertook the whole genome sequencing of Australian
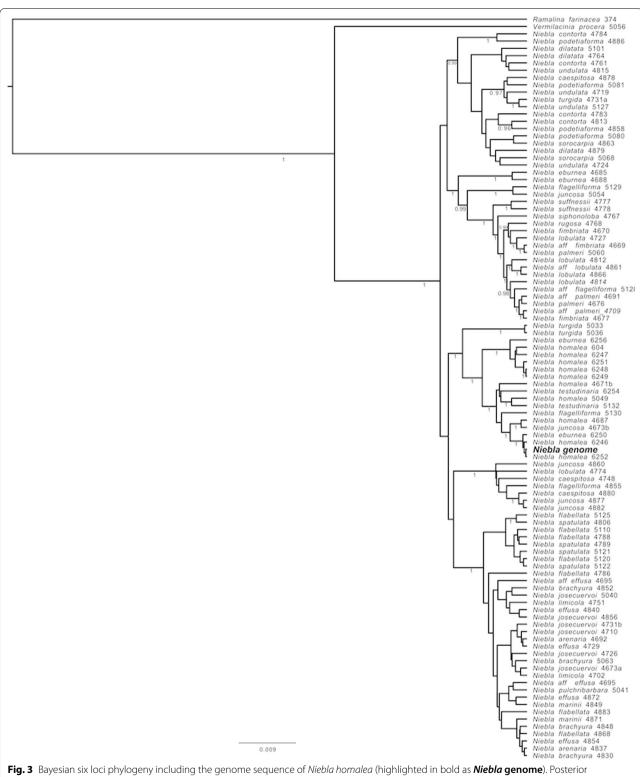
Fig. 3 Bayesian six loci phylogeny including the genome sequence of *Niebla homalea* (highlighted in bold as **Niebla genome**). Posterior probability values above 0.95 are indicated below the branches. *Ramalina farinacea* and *Vermilacinia procera* were used as outgroup

Duong *et al. IMA Fungus* (2021) 12:30

Page 10 of 17

field collected hybrid, WAC10721. WAC10721 was characterised as a hybrid based on amplified fragment length polymorphism and *P. teres* form specific PCR markers (McLean et al. 2014; Poudel et al. 2017).

Sequenced strain
Australia: *Western Australia*: Esperance, isolated from *Hordeum vulgare*, Dec. 2002, *S. Gupta* WAC10721 (BRIP71571).

Nucleotide sequence accession number
This whole-genome shotgun project has been deposited in NCBI GenBank database under accession number JACXVK000000000 (BioProject: PRJNA656142 and BioSample: SAMN15768574). This paper describes the first version of this genome.

Materials and methods
Genomic DNA of WAC10721 was extracted from 10-day-old mycelium using a Wizard® Genomic DNA Purification kit (Promega, Sydney, Australia) as per the manufacturer's protocol. The DNA was sent to Australian Genome Research Facility (AGRF), Melbourne, where integrity of DNA samples was confirmed by Agilent 2100 Bioanalyzer, agarose gel electrophoresis, and NanoDrop^TC 2000/2000c. The shotgun DNA library was constructed by AGRF as per Illumina's protocol and sequenced with 125 bp pair-end reads on Illumina HiSeq 2000. The sequence quality of the pair-end reads were examined using FastQC (Galaxy v.0.72) (Afgan et al. 2018).

The adapter sequences were removed and reads with average phred score lower than 30 bp were filtered in the CLC Genomics Workbench v9.5.4 (hereafter referred to as CLC). De novo whole genome assembly was performed in CLC by adjusting word size from 20 to 40 bp using CLC default parameters (Arun-Chinnappa and McCurdy 2015; Henkel et al. 2012). Assembly quality was assessed using QUAST v5.0.2 (Gurevich et al. 2013). Repeat elements were detected and then masked using RepeatModeler v1.0.11 with Repbase v20.4 library (Bao et al. 2015) and RepeatMasker v4.0.9, respectively (http://www.repeatmasker.org).

For de novo gene annotation, the first round of MAKER2 v2.31.10 (Holt and Yandell 2011) was completed with AUGUSTUS v3.3.3 (Stanke et al. 2006a, b) using model organisms *Neurospora crassa* as training set and a self-trained GeneMark-ES v4.46 (Ter-Hovhannisyan et al. 2008) along with coding DNA and protein sequences of *P. teres* f. *teres* 0–1 (Ellwood et al. 2010) as gene and protein evidences. The gene models obtained from the first MAKER2 run were then used to train the ab initio annotation program SNAP (Korf 2004) and the

second round of MAKER2 was rerun with a SNAP training output was used in the second round of Maker to further refine gene models. BUSCO v.4.1.2 (Simão et al. 2015) with fungi_odb10 database (758 core genes) was used to evaluate the completeness of the genome assembly. Interproscan v5.38-76.0 (Jones et al. 2014) was used to functionally annotate the predicted proteins and to assign gene ontology (GO) terms for the annotation data.

OrthoFinder v2.3.3 (Emms and Kelly 2015) was used to cluster the predicted proteins into orthologous groups together with *P. teres* f. *teres* and *P. teres* f. *maculata* proteomes (W1-1 and SG1) (Syme et al. 2018). SignalP v5.0 (Armenteros et al. 2019) and TMHMM v2.0 (Chen et al. 2003) were used to identify signal peptide and transmembrane domains in the predicted proteins. The proteins with the presence of a signal peptide and zero or one transmembrane domains were subjected to effector identification using EffectorP v2.0 (Sperschneider et al. 2018). The secondary metabolites were predicted using the assembly as input to the web-based antiSMASH 2.0 (Blin et al. 2017).

Results and discussion
Illumina sequencing generated 50 million reads on average accounting for $\sim 100 \times$ coverage of the whole genome. The genome was assembled into 2128 contigs that were equal to or larger than 500 bp. Total assembly length was 34.9 Mb with a GC content of 49.48% and a N_{50} value of 343,074. The longest contig consisted of 1,776,994 bp. We identified 1891 long terminal repeats, 695 DNA elements, 56 long interspersed nuclear elements, 4264 unclassified repeats, 7403 simple repeats and 750 low complexity regions. Repeats constituted of 10.54% of the genome. A total of 10,835 protein coding genes were predicted. BUSCO was used to assess the WAC10721 genome completeness and 98.6% of the core genes of fungi were identified. The basic statistics of assembly, repeat content and gene number for the reference genome of *P. teres* f. *teres* (W1-1), *P. teres* f. *maculata* (SG1) and the hybrid genome (WAC10721) are reported in Table 2. A phylogenetic tree reflecting the position of this genome in relation to other analysis of the genus *Pyrenophora* species is presented in Fig. 4.

The hybrid WAC10721 genome had 10,051 genes and these grouped in 9667 orthologous groups. In total, 9378 orthologous groups were common to all three isolates and WAC10721 shared 167 and 122 unique orthologous genes with the *P. teres* f. *teres* and *P. teres* f. *maculata* reference genome, respectively. Effector proteins and secondary metabolites play important roles in fungal pathogenicity and virulence (Moolhuijzen et al. 2020; Muria-Gonzalez et al. 2020; Wyatt et al. 2020). A total of 1039 predicted proteins in the genome have

Duong *et al. IMA Fungus*   (2021) 12:30

Page 11 of 17

secretion signals and 18 of those were identified as effectors. In total 25 secondary metabolite gene clusters were identified comprising of 17 non-ribosomal peptide synthetases (NRPS), 14 polyketide synthases (PKS), three terpene and eight unclassified clusters. Files with information about the genome annotation, functional prediction, repeats, effectors and orthologous genes have been deposited on Zenodo with the DOI number (https://doi.org/10.5281/zenodo.4107533). This is the first report of the genome of a *P. teres* hybrid. The data produced here will be useful for comparative genomics studies to understand differences between two forms of *P. teres* and hybrids and for investigating the mechanism of the pathogenicity of the species.

Authors: **Barsha Poudel, Kiruba Shankari Arun-Chinnappa, Anke Martin**[*]

*Contact: Anke.Martin@usq.edu.au

IMA GENOME – F 15E

A low coverage draft genome of the *Eucalyptus* leaf blight pathogen *Teratosphaeria viscida*
Introduction

Teratosphaeria viscida is one of a number of *Teratosphaeria* species that have emerged as pathogens of planted *Eucalyptus* trees over the past few decades (Burgess and Wingfield 2017, Andjic et al. 2019, Aylward et al. 2019). Unlike some other species, which are economically important globally, *T. viscida* is currently only known from *Eucalyptus* trials in tropical northern Queensland, Australia, where it has caused disease on *E. grandis* and *E. grandis* × *E. camaldulensis* trees (Andjic et al. 2007). Leaf blight caused by *T.*

Table 2 Genomic Statistics of the reference genome of *Pyrenophora teres* f. *teres* (W1-1), *P. teres* f. *maculata* (SG1) and the hybrid genome, WAC10721

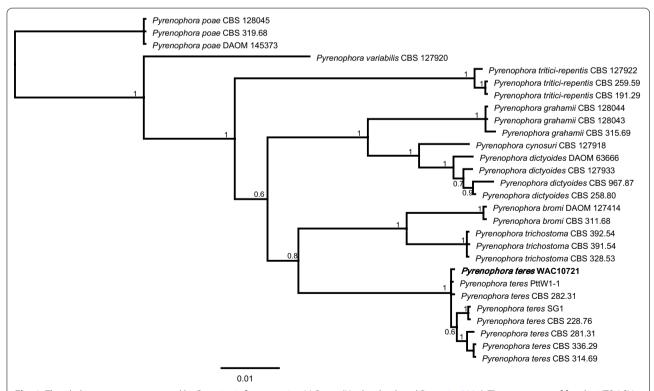| Genomic statistics	Values		
	W1-1	**SG1**	**WAC10721**
Assembly size (Mbp)	51.76	41.28	34.90
Number of contigs (=> 500 bp)	74	47	2,128
N_{50} (bp)	3,700,000	2,110,000	343,074
GC-content (%)	45.21	46.86	49.48
Repeat Elements (bp)	3,115,060	1,061,852	3,419,914
Genes	11,245	11,165	10,835

Fig. 4 The phylogeny was constructed by Bayesian inference using MrBayes (Huelsenbeck and Ronquist 2001). The sequences of four loci ITS, LSU, *gapdh* and *tef1* were either obtained from the study of Marin-Felix et al. (2019), or extracted from the reference genome of *Pyrenophora teres* from Syme et al. (2018). Sequence alignments were produced using MAFFT v.7 (Katoh and Standley 2013)

Duong *et al. IMA Fungus*   (2021) 12:30

Page 12 of 17

viscida was of particular concern when it was first identified because both the climatic conditions and host symptoms closely resembled those associated with disease outbreaks caused by *T. destructans*, one of the most devastating *Eucalyptus* foliar pathogens (Wingfield et al. 1996, Havenga et al. 2021).

On native *E. grandis* in Australia, *T. viscida* does not appear to be an aggressive pathogen, affecting < 15% of foliage and damaging only foliage in the lower tree canopy (Andjic et al. 2007). In contrast, an *E. grandis* × *E. camaldulensis* hybrid that was developed in South America and planted in Queensland became heavily infected within a year, with defoliation exceeding 95% (Andjic et al. 2007). These hybrid trees, stressed due to damage by *T. viscida*, were subsequently severely infected by *T. epicoccoides*, a species that typically causes only minor symptoms in healthy trees (Gardner and Hodges 1988, Taole et al. 2015, Andjic et al. 2019).

Phylogenetic studies have shown that *T. viscida* is closely related to other *Teratosphaeria* foliar pathogens that have asexual states in the genus *Kirramyces* (Andjic et al. 2019). These include *T. destructans*, a devastating pathogen across South East Asia and South Africa (Greyling et al. 2016, Havenga et al. 2021), and two other species, *T. novaehollandiae* and *T. tiwiana*, known only from Australia (Andjic et al. 2016). The aim of this study was to sequence the genome of *T. viscida*, as the closest relative of *T. destructans* with a genome available for comparative studies. Comparing the genome of *T. viscida* to those of aggressive pathogens such as *T. destructans* and *T. pseudoeucalypti* (Andjic et al. 2010) will also enable evaluation of the risk that this species poses as a potentially damaging pathogen of planted *Eucalyptus*.

Sequenced strain
Australia: *Queensland*: Mareeba, isolated from leaf spots on a *Eucalyptus grandis*, 2005, *T.I. Burgess* (CMW51324 = CBS121156 – culture).

Nucleotide accession number
The genomic sequence of *T. viscida* has been deposited at DDJ/EMBL/GenBank under the accession JAHESH000000000. This paper describes the first version.

Materials and methods
The culture of *T. viscida* is maintained in the culture collection (CMW) of the Forestry and Agricultural Biotechnology Institute (FABI), University of Pretoria, and the Westerdijk Fungal Biodiversity Institute (CBS), Utrecht, Netherlands. The isolate was grown on malt extract agar (Merck, Wadeville, South Africa) at 25 °C in the dark, until sufficient mycelia was available for DNA extraction, following methods previously described for *Teratosphaeria* species (Wingfield et al. 2018, Wilken et al. 2020). Extracted DNA was submitted to Inqaba Biotec (Pretoria, South Africa) for low coverage sequencing on the PacBio Sequel II System and to Macrogen (Seoul, Korea) for sequencing on the Illumina HiSeq 2500 platform. One Illumina paired-end library, with an insert size of 550 bp, was sequenced at a target read-length of 250 bp.

The quality of the raw Illumina sequence reads was assessed with FastQC 0.11.5 (Andrews 2010) and trimming was performed with Trimmomatic 0.38 (Bolger et al. 2014). Trimmed Illumina reads were assembled with SPAdes 3.14.0 (Bankevich et al. 2012), applying the "careful" option. Scaffolding was performed by aligning the PacBio reads to the SPAdes assembly with Minimap 2.17 (Li 2018) and running the Long Reads Scaffolder 1.1.11 (LRScaf; Qin et al. 2019). Both the Illumina and PacBio raw reads were used for final error correction of the hybrid assembly in Pilon 1.22 (Walker et al. 2014a, b). The completeness of the error-corrected assembly was assessed with BUSCO 4.1.4 using the Fungi *odb10* dataset (Simão et al. 2015). Repeat identification and gene prediction with the MAKER 2.31.10 pipeline (Holt and Yandell 2011) followed the method used for *T. gauchensis* and *T. zuluensis* (Wingfield et al. 2019). The *MAT1* locus of *T. viscida* was identified with BLASTn using the *MAT1* idiomorphs of *T. zuluensis* (GenBank accessions MN119556 and MN119557).

To confirm the taxonomic position of the *T. viscida* genome isolate, the Beta-tubulin, translation elongation factor-1 α (EF-1α) and internal transcribed spacer (ITS) regions were extracted from the genome. These were included in a maximum likelihood phylogeny with GenBank-obtained sequences from the ex-type isolates of other closely related *Teratosphaeria* leaf pathogens, using the two stem canker pathogens, *T. gauchensis* and *T. zuluensis*, as outgroup species. All sequences were aligned independently with MAFFT 7.407 (Katoh and Standley 2013), trimmed with trimAl 1.4.rev22 (Capella-Gutiérrez et al. 2009) and the best substitution model determined with ModelTest-NG 0.1.6 (Darriba et al. 2020) using the Akaike information criterion (AIC). Maximum likelihood (ML) phylogenies of the individual nucleotide alignments were constructed in RAxML-NG 1.0.2 (Kozlov et al. 2019), applying 1000 bootstrap replicates. A concatenated ML phylogeny was reconstructed after confirming congruence among the gene trees.

Results and discussion
Illumina sequencing yielded 1.6 million paired-end reads of which 68.9% were retained as paired and 13.3%

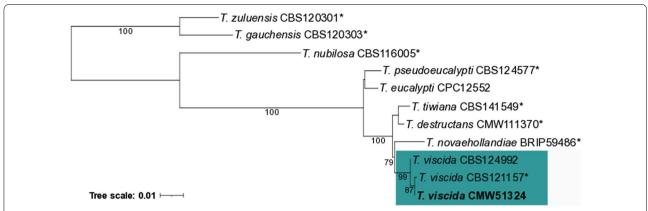Duong *et al. IMA Fungus* (2021) 12:30

Page 13 of 17

Fig. 5 Maximum likelihood phylogeny of the concatenated Beta-tubulin, EF-1α and ITS gene regions indicating the taxonomic position of the *Teratosphaeria viscida* genome isolate (bold). Type isolates are indicated with an asterisk (*). Support values represent the transfer bootstrap expectation metric (TBE) of Lemoine et al. (2018). GenBank accession numbers are available in Quaedvlieg et al. (2014) and Andjic et al. (2016)

as single reads after quality trimming. Mean length for the 38,050 PacBio reads was 3.8 kb, representing approximately 5X genome coverage. The final error-corrected hybrid genome assembly was 37.4 Mb, with an estimated coverage of 14X, a GC content of 49.1% and a BUSCO completeness score of 98.7%. It consisted of 1879 contigs with an N50 and L50 of 130 kb and 83 contigs, respectively. The size of the *T. viscida* genome was 6–11 Mb larger than that of other published *Teratosphaeria* genome assemblies (Wingfield et al. 2018, 2019; Havenga et al. 2020; Wilken et al. 2020), a characteristic reflected in its 28.7% repetitive fraction. Up to this point, the highest estimated repeat content for a *Teratosphaeria* pathogen had been approximately 17% for *T. destructans* (Wingfield et al. 2019; Wilken et al. 2020). The number of predicted genes (9528) for *T. viscida* was similar to that of other *Teratosphaeria* species.

ML analysis of three concatenated barcoding genes confirmed that the genome strain resolves in a well-supported monophyletic clade with the ex-type strain of *T. viscida* (Fig. 5). It also confirmed the close relationship among *T. viscida* and the other species, *T. destructans*, *T. novaehollandiae* and *T. tiwiana*, having kirramyces-like conidia. BLASTn identified a *MAT1-1* idiomorph in the *T. viscida* genome, with the same gene content and flanking genes as that of *T. zuluensis* (Aylward et al. 2020). *Teratosphaeria viscida* is, therefore, heterothallic, similar to most other investigated *Teratosphaeria* species, the exception in this case being *T. nubilosa* (Hunter et al. 2009).

The genome sequence derived from *T. viscida* in this study is the first for a *Teratosphaeria* species that is apparently less aggressive than its closest relatives. Additionally, it is the only genome from a species known exclusively from eastern Australia. The genome of this species is a valuable addition to the dataset of *Teratosphaeria* genomes and will be a useful comparison with aggressive leaf pathogens for which genomes are already available, including *T. destructans*, *T. pseudoeucalypti* and *T. nubilosa* (Wingfield et al. 2018, Haridas et al. 2020, Wilken et al. 2020).

Authors: **Janneke Aylward***, **Brenda D. Wingfield, Michael J. Wingfield**
**Contact:* janneke.aylward@fabi.up.ac.za

Duong *et al. IMA Fungus* (2021) 12:30

Page 14 of 17

Declarations

Ethics approval and consent to participate
Not applicable.

Adherence to national and international regulations
Not applicable.

Consent for publication
Not applicable.

Competing interests
The authors declare that they have no competing interests.

Author details
[1]Department of Biochemistry, Genetics and Microbiology, Forestry and Agricultural Biotechnology Institute (FABI), University of Pretoria, Private Bag X20, Hatfield 0028, South Africa. [2]Department of Conservation Ecology and Entomology, Stellenbosch University, Private Bag X1, Matieland 7602, South Africa. [3]Field Museum, Department of Science and Education, Grainger Bioinformatics Center, 1400 S Lake Shore Drive, Chicago, IL 60605, USA. [4]Centre for Crop Health, University of Southern Queensland, Toowoomba, QLD 4350, Australia. [5]Biotechnology Platform, Agricultural Research Council, Onderstepoort, Pretoria 0110, South Africa. [6]PerkinElmer Pty LTD., Level 2, Building 5, Brandon Business Park 530-540, Springvale Road, Glen Waverley, VIC 3150, Australia.

References
Afgan E, Baker D, Batut B, van den Beek M, Bouvier D et al (2018) The Galaxy platform for accessible, reproducible and collaborative biomedical analyses: 2018 update. Nucleic Acids Res 46:W537–W544

Afgan E, Baker D, van den Beek M, Blankenberg D, Bouvier D et al (2016) The Galaxy platform for accessible, reproducible and collaborative biomedical analyses: 2016 update. Nucleic Acids Res 44(W1):W3–W10

Andjic V, Barber PA, Carnegie AJ, Pegg GS, Hardy GSJ et al (2007) *Kirramyces viscidus* sp. nov., a new eucalypt pathogen from tropical Australia closely related to the serious leaf pathogen *Kirramyces Destructans*. Australasian Plant Pathol 36:478–487

Andjic V, Carnegie AJ, Pegg GS, Hardy GESJ, Maxwell A et al (2019) 23 years of research on *Teratosphaeria* leaf blight of Eucalyptus. For Ecol Manag 443:19–27

Andjic V, Maxwell A, Hardy GESJ, Burgess TI (2016) New cryptic species of *Teratosphaeria* on Eucalyptus in Australia. IMA Fungus 7:253–263

Andjic V, Pegg GS, Carnegie AJ, Callister A, Hardy GE et al (2010) *Teratosphaeria pseudoeucalypti*, new cryptic species responsible for leaf blight of Eucalyptus in subtropical and tropical Australia. Plant Pathol 59:900–912

Andrews S (2010) FastQC: a quality control tool for high throughput sequence data [Online]. http://www.bioinformatics.babraham.ac.uk/projects/fastqc/. In.: Babraham Bioinformatics, Babraham Institute, Cambridge, UK

Anisimova M, Gascuel O (2006) Approximate likelihood-ratio test for branches: a fast, accurate, and powerful alternative. Syst Biol 55:539–552

Armenteros JJA, Tsirigos KD, Sonderby CK, Petersen TN, Winther O, Brunak S, von Heijne G, Nielsen H (2019) SignalP 5.0 improves signal peptide predictions using deep neural networks. Nat Biotechnol 37:420–423

Arun-Chinnappa KS, McCurdy DW (2015) De novo assembly of a genome-wide transcriptome map of *Vicia faba* (L.) for transfer cell research. Front Plant Sci 6:217–217

Aylward J, Havenga M, Dreyer LL, Roets F, Wingfield BD et al (2020) Genomic characterization of mating type loci and mating type distribution in two apparently asexual plantation tree pathogens. Plant Pathol 69:28–37

Aylward J, Roets F, Dreyer LL, Wingfield MJ (2019) *Teratosphaeria* stem canker of Eucalyptus: two pathogens, one devastating disease. Mol Plant Pathol 20:8–19

Bankevich A, Nurk S, Antipov D, Gurevich AA, Dvorkin M et al (2012) SPAdes: a new genome assembly algorithm and its applications to single-cell sequencing. J Comput Biol 19:455–477

Bao WD, Kojima KK, Kohany O (2015) Repbase update, a database of repetitive elements in eukaryotic genomes. Mobile DNA-Uk 6

Batra LR (1963) Ecology of ambrosia fungi and their dissemination by beetles. Trans Kans Acad Sci 66:213–223

De Beer ZW, Duong TA, Barnes I, Wingfield BD, Wingfield MJ (2014) Redefining *Ceratocystis* and allied genera. Stud Mycol 79:187–219

Blin K, Shaw S, Steinke K, Villebro R, Ziemert N, Lee S et al (2019) antiSMASH 5.0: updates to the secondary metabolite genome mining pipeline. Nucleic Acids Res 47:W81–W87

Blin K, Wolf T, Chevrette MG, Lu XW, Schwalen CJ et al (2017) antiSMASH 4.0-improvements in chemistry prediction and gene cluster boundary identification. Nucleic Acids Res 45:W36–W41

Bolger A, Lohse M, Usadel B (2014) Trimmomatic: a flexible trimmer for Illumina sequence data. Bioinformatics 30:2114–2120

Bouckaert R, Heled J, Kuhnert D, Vaughan T, Wu C et al (2014) BEAST 2: a software platform for Bayesian evolutionary analysis. PLoS Comput Biol 10:e1003537

Browne P, Nielsen T, Kot W, Aggerholm A, Gilbert M et al (2020) GC bias affects genomic and metagenomic reconstructions, underrepresenting GC-poor organisms. GigaScience 9(2):giaa008

Burgess TI, Wingfield MJ (2017) Pathogens on the move: a 100-year global experiment with planted Eucalypts. Bioscience 67:14–25

Campbell GF, Crous PW (2003) Genetic stability of net x spot hybrid progeny of the barley pathogen *Pyrenophora teres*. Australasian Plant Pathol 32:283–287

Campbell GF, Crous PW, Lucas JA (1999) *Pyrenophora teres* f. *maculata*, the cause of *Pyrenophora* leaf spot of barley in South Africa. Mycol Res 103:257–267

Campbell GF, Lucas JA, Crous PW (2002) Evidence of recombination between net- and spot-type populations of *Pyrenophora teres* as determined by RAPD analysis. Mycol Res 106:602–608

Cantarel B, Korf I, Robb S, Parra G, Ross E, Moore B et al (2008) MAKER: an easy-to-use annotation pipeline designed for emerging model organism genomes. Genome Res 18:188–196

Capella-Gutiérrez S, Silla-Martínez JM, Gabaldón T (2009) trimAl: a tool for automated alignment trimming in large-scale phylogenetic analyses. Bioinformatics 25:1972–1973

Castresana J (2000) Selection of conserved blocks from multiple alignments for their use in phylogenetic analysis. Mol Biol Evol 17:540–552

Chen YJ, Yu P, Luo JC, Jiang Y (2003) Secreted protein prediction system combining CJ-SPHMM, TMHMM, and PSORT. Mamm Genome 14:859–865

Darriba D, Posada D, Kozlov AM, Stamatakis A, Morel B, Flouri T (2020) ModelTest-NG: a new and scalable tool for the selection of DNA and protein evolutionary models. Mol Biol Evol 37:291–294

Darribo D, Taboada GL, Doallo R, Posada D (2012) jModelTest 2: More models, new heuristics and parallel computing. Nat Methods 9:772

Dereeper A, Audic S, Claverie JM, Blanc G (2010) BLAST-EXPLORER helps you building datasets for phylogenetic analysis. BMC Evol Biol 10:8

Dereeper A, Guignon V, Blanc G, Audic S, Buffet S, Chevenet F, Dufayard JF, Guindon S, Lefort V, Lescot M, Claverie JM, Gascuel O (2008) Phylogeny.fr: robust phylogenetic analysis for the non-specialist. Nucleic Acids Res 36:W465–W469

Edgar RC (2004) MUSCLE: multiple sequence alignment with high accuracy and high throughput. Nucleic Acids Res 32(5):1792–1797

Ellwood SR, Liu Z, Syme RA, Lai Z, Hane JK, Keiper F, Moffat CS, Oliver RP, Friesen TL (2010) A first genome assembly of the barley fungal pathogen Pyrenophora teres f. teres. Genome Biol 11:R109

Emms DM, Kelly S (2015) OrthoFinder: solving fundamental biases in whole genome comparisons dramatically improves orthogroup inference accuracy. Genome Biol 16:16

Fourie A, van der Nest MA, de Vos L, Wingfield MJ, Wingfield BD et al (2019) QTL mapping of mycelial growth and aggressiveness to distinct hosts in *Ceratocystis* pathogens. Fungal Genet Biol 131:103242

Gardner DE, Hodges CS (1988) Hawaiian Forest Fungi. IX. *Botryosphaeria pipturi* sp. nov. and Miscellaneous Records. Mycologia 80:460–465

Green T, Sancho L, Pintado A (2011) Ecophysiology of desiccation/rehydration cycles in mosses and lichens. In: Plant desiccation tolerance, pp 89–120

Duong *et al. IMA Fungus*   (2021) 12:30

Page 15 of 17

Greyling I, Wingfield MJ, Coetzee MPA, Marincowitz S, Roux J (2016) The Eucalyptus shoot and leaf pathogen *Teratosphaeria destructans* recorded in South Africa. Southern for 78:123–129

Guindon S, Dufayard J-F, Lefort V, Anisimova M, Hordijk W et al (2010) New algorithms and methods to estimate maximum-likelihood phylogenies: assessing the performance of PhyML 3.0. Syst Biol 59:307–321

Guindon S, Gascuel O (2003) A simple, fast, and accurate algorithm to estimate large phylogenies by maximum likelihood. Syst Biol 52:696–704

Gurevich A, Saveliev V, Vyahhi N, Tesler G (2013) QUAST: quality assessment tool for genome assemblies. Bioinformatics 29:1072–1075

Haridas S, Albert R, Binder M, Bloem J, Labutti K et al (2020) 101 Dothideomycetes genomes: a test case for predicting lifestyles and emergence of pathogens. Stud Mycol 96:141–153

Harrington TC, Aghayeva DN, Fraedrich SW (2010) New combinations in Raffaelea, Ambrosiella, and Hyalorhinocladiella, and four new species from the redbay ambrosia beetle, Xyleborus glabratus. Mycotaxon 111:337–361

Harrington TC, McNew D, Mayers C, Fraedrich SW, Reed SE (2014) *Ambrosiella roeperi* sp. nov. is the mycangial symbiont of the granulate ambrosia beetle *Xylosandrus Crassiusculus*. Mycologia 106:835–845

Harrington TC (2005) Ecology and evolution of mycophagous bark beetles and their fungal partners. In: Vega FE, Blackwell M (eds) Ecological and evolutionary advances in insect-fungal associations. Oxford University Press, New York, pp 257–291

Havenga M, Wingfield BD, Wingfield MJ, Marincowitz S, Dreyer LL et al (2021) Genetic recombination in *Teratosphaeria destructans* causing a new disease outbreak in Malaysia. For Pathol 51:e12683

Havenga M, Wingfield BD, Wingfield MJ, Roets F, Dreyer LL et al (2020) Mating strategy and mating type distribution in six global populations of the Eucalyptus foliar pathogen *Teratosphaeria destructans*. Fungal Genet Biol 137:103350

Henkel CV, Dirks RP, de Wijze DL, Minegishi Y, Aoyama J et al (2012) First draft genome sequence of the Japanese eel, *Anguilla japonica*. Gene 511:195–201

Herron DA, Wingfield MJ, Rodas CA, Marincowitz S, Steenkamp ET (2015) Novel taxa in the *Fusarium fujikuroi* species complex from *Pinus* spp. Stud Mycol 80:131–150

Holt C, Yandell M (2011) MAKER2: an annotation pipeline and genome-database management tool for second-generation genome projects. BMC Bioinform 12:491

Huelsenbeck JP, Ronquist F (2001) MRBAYES: Bayesian inference of phylogenetic trees. Bioinformatics 17:754–755

Hunter GC, Crous PW, Carnegie AJ, Wingfield MJ (2009) *Teratosphaeria nubilosa,* a serious leaf disease pathogen of Eucalyptus spp. in native and introduced areas. Mol Plant Pathol 10:1–14

Jalli M (2011) Sexual reproduction and soil tillage effects on virulence of *Pyrenophora teres* in Finland. Ann Appl Biol 158:95–105

Jones P, Binns D, Chang H, Fraser M, Li W et al (2014a) InterProScan 5: genome-scale protein function classification. Bioinformatics 30:1236–1240

Katoh K, Rozewick J, Yamada KD (2019) MAFFT online service: multiple sequence alignment, interactive sequence choice and visualization. Brief Bioinform 20:1160–1166

Katoh K, Standley DM (2013) MAFFT multiple sequence alignment software version 7: improvements in performance and usability. Mol Biol Evol 30:772–780

Keller O, Kollmar M, Stanke M, Waack S (2011) A novel hybrid gene prediction method employing protein multiple sequence alignments. Bioinformatics 27:757–763

Kirisits T (2004) Fungal associates of European bark beetles with special emphasis on the ophiostomatoid fungi. In: Bark and wood boring insects in living trees in Europe, a synthesis. Springer, pp 181–236

Kistenich S, Timdal E, Bendiksby M, Ekman S (2018) Molecular systematics and character evolution in the lichen family Ramalinaceae (Ascomycota: Lecanorales). Taxon 67:871–904

Kolmogorov M, Yuan J, Lin Y, Pevzner PA (2019) Assembly of long, error-prone reads using repeat graphs. Nat Biotechnol 37:540–546

Koren S, Walenz B, Berlin K, Miller J, Bergman N et al (2017a) Canu: scalable and accurate long-read assembly via adaptive k-mer weighting and repeat separation. Genome Res 27:722–736

Korf I (2004) Gene finding in novel genomes. BMC Bioinform 5:59

Kozlov AM, Darriba D, Flouri T, Morel B, Stamatakis A (2019) RAxML-NG: a fast, scalable and user-friendly tool for maximum likelihood phylogenetic inference. Bioinformatics 35:4453–4455

Kvas M, Marasas WFO, Wingfield BD, Wingfield MJ, Steenkamp ET (2009) Diversity and evolution of *Fusarium* species in the *Gibberella fujikuroi* complex. Fungal Divers 34:1–21

Lemoine F, Entfellner J-BD, Wilkinson E, Correia D, Felipe MD, Oliveira TD, Gascuel O (2018) Renewing Felsenstein's phylogenetic bootstrap in the era of big data. Nature 556:452

Li H (2018) Minimap2: pairwise alignment for nucleotide sequences. Bioinformatics 34:3094–3100

Li H, Durbin R (2009) Fast and accurate short read alignment with Burrows–Wheeler transform. Bioinformatics 25:1754–1760

Li H, Durbin R (2010) Fast and accurate long-read alignment with Burrows–Wheeler transform. Bioinformatics 265:589–595

Liu Z, Ellwood SR, Oliver RP, Friesen TL (2011) *Pyrenophora teres*: profile of an increasingly damaging barley pathogen. Mol Plant Pathol 12:1–19

Lopez-Ruiz F, Mair W, Thomas G, Jayasena KW, Hills A, Martin A (2020) Azole resistance in spot-form net blotch in Western Australia. Grains Research and Development Corporation, Australia

Ma L-J, Van der Does HC, Borkovich KA, Coleman JJ, Daboussi M-J et al (2010) Comparative genomics reveals mobile pathogenicity chromosomes in *Fusarium*. Nature 464:367–373

Marin-Felix Y, Hernández-Restrepo M, Iturrieta-González I, García DG et al (2019) Genera of phytopathogenic fungi: GOPHY 3. Stud Mycol 94:1–124

Martin M (2011) Cutadapt removes adapter sequences from high-throughput sequencing reads. Embnet J 17(1):3

Massoumi Alamouti S, Tsui CKM, Breuil C (2009) Multigene phylogeny of filamentous ambrosia fungi associated with ambrosia and bark beetles. Mycol Res 113:822–835

Mathre DE (1982) Compendium of barley diseases. American Phytopathological Society in cooperation with the Department of Plant Pathology Montana State University, St. Paul, Minn

Mayers CG, Bateman CC, Harrington TC (2018) New *Meredithiella* species from mycangia of Corthylus ambrosia beetles suggest genus-level coadaptation but not species-level coevolution. Mycologia 110:63–78

Mayers CG, Harrington TC, Masuya H, Jordal BH, McNew DL et al (2020) Patterns of coevolution between ambrosia beetle mycangia and the Ceratocystidaceae, with five new fungal genera and seven new species. Persoonia 44:41–66

Mayers CG, McNew DL, Harrington TC, Roeper RA, Fraedrich SW et al (2015) Three genera in the Ceratocystidaceae are the respective symbionts of three independent lineages of ambrosia beetles with large, complex mycangia. Fungal Biol 119:1075–1092

McKenzie S, Walston R, Allen J (2020) Complete, high-quality genomes from long-read metagenomic sequencing of two wolf lichen thalli reveals enigmatic genome architecture. Genomics 112:3150–3156

McLean MS, Howlett BJ, Hollaway GJ (2009) Epidemiology and control of spot form of net blotch (*Pyrenophora teres* f. *maculata*) of barley: a review. Crop Pasture Sci 60:303–315

McLean MS, Martin A, Gupta S, Sutherland MW, Hollaway GJ, Platz GJ (2014) Validation of a new spot form of net blotch differential set and evidence for hybridisation between the spot and net forms of net blotch in Australia. Austral Plant Pathol 43:223–233

Mikheenko A, Prjibelski A, Saveliev V, Antipov D, Gurevich A (2018) Versatile genome assembly evaluation with QUAST-LG. Bioinformatics 34(13):i142–i150

Montagne D (1852) Diagnoses Phycologicae. Ann Sci Nat Sr 18(3):302–319

Moolhuijzen PM, Muria-Gonzalez MJ, Syme R, Rawlinson C, See PT, Moffat CS, Ellwood SR (2020) Expansion and conservation of biosynthetic gene clusters in pathogenic *Pyrenophora* spp. Toxins 12:242

Muria-Gonzalez MJ, Zulak KG, Allegaert E, Oliver RP, Ellwood SR (2020) Profile of the in vitro secretome of the barley net blotch fungus, *Pyrenophora teres* f. teres. Physiol Mol Plant P 109:101451

Möller EM, Bahnweg G, Sandermann H, Geiger HH (1992) A simple and efficient protocol for isolation of high molecular weight DNA from filamentous fungi, fruit bodies, and infected plant tissues. Nucleic Acids Res 20:6115–6116

Duong *et al. IMA Fungus* (2021) 12:30

Page 16 of 17

Nel WJ, de Beer ZW, Wingfield MJ, Duong TA (2020) The granulate ambrosia beetle, *Xylosandrus crassiusculus* (Coleoptera: Curculionidae, Scolytinae), and its fungal symbiont found in South Africa. Zootaxa 4838:427–435

Van der Nest MA, Steenkamp ET, Roodt D, Soal NC, Palmer M et al (2019) Genomic analysis of the aggressive tree pathogen *Ceratocystis albifundus*. Fungal Biol 123:351–363

Niehaus E-M, Münsterkötter M, Proctor RH, Brown DW, Sharon A et al (2017) Comparative "omics" of the *Fusarium fujikuroi* species complex highlights differences in genetic potential and metabolite synthesis. Genome Biol Evol 8:3574–3599

O'Donnell K, Cigelnik E, Nirenberg HI (1998) Molecular systematics and phylogeography of the *Gibberella fujikuroi* species complex. Mycologia 90:465–493

O'Donnell K, Nirenberg HI, Aoki T, Cigelnik E (2000) A multigene phylogeny of the *Gibberella fujikuroi* species complex: detection of additional phylogenetically distinct species. Mycoscience 41:61–78

Park S, Choi J, Lee G, Kim J, Oh S, Jeong M et al (2014) Draft genome sequence of lichen-forming fungus Cladonia metacorallifera strain KoLRI002260. Genome Announc 2:e01065-e1113

Poudel B, Ellwood SR, Testa AC, McLean M, Sutherland MW et al (2017) Rare *Pyrenophora teres* hybridization events revealed by development of sequence-specific PCR markers. Phytopathology 107:878–884

Poudel B, McLean MS, Platz GJ, McIlroy JA, Sutherland MW et al (2018) Investigating hybridisation between the forms of *Pyrenophora teres* based on Australian barley field experiments and cultural collections. Eur J Plant Pathol 153:465–473

Qin M, Wu S, Li A, Zhao F, Feng H, Ding L, Ruan J (2019) LRScaf: improving draft genomes using long noisy reads. BMC Genomics 20:955

Quaedvlieg W, Binder M, Groenewald JZ, Summerell BA, Carnegie AJ, Burgess TI, Crous PW (2014) Introducing the consolidated species concept to resolve species in the Teratosphaeriaceae. Persoonia 33:1–40

Rambaut A, Drummond AJ, Xie D, Baele Suchard MA (2018) Posterior summarization in Bayesian phylogenetics using Tracer 1.7. Syst Biol 67:901

Rundel P (1978b) Ecological relationships of desert fog zone lichens. Bryologist 81:277–293

Rundel P (1978a) Niebla, a new generic name for the lichen genus Desmazieria (Ramalinaceae). Mycotaxon 6:497–499

Rundel P, Bowler P, Mulroy T (1972) A fog-induced lichen community in Northwestern Baja California, with two new species of Desmazieria. Bryologist 72:501–508

Rundel P, Dillon M, Palma B, Mooney H, Gulmon S et al (1991) The phytogeography and ecology of the coastal Atacama and Peruvian deserts. Aliso 13:1–49

Seppey M, Manni M, Zdobnov EM (2019) BUSCO: Assessing genome assembly and annotation completeness. In: Kollmar M (ed) Gene prediction: methods and protocols, methods in molecular biology. Humana, New York

Simão FA, Waterhouse RM, Ioannidis P, Kriventseva EV, Zdobnov EM (2015) BUSCO: assessing genome assembly and annotation completeness with single-copy orthologs. Bioinformatics 31:3210–3212

Six DL (2003) Bark beetle-fungus symbiosis. In: Bourtzis K, Miller TA (eds) Insect symbiosis. CRC Press, Washington, DC, p 97

Skelton J, Jusino MA, Li Y, Bateman C, Thai PH, Wu C, Lindner DL, Hulcr J (2018) Detecting symbioses in complex communities: the fungal symbionts of bark and ambrosia beetles within Asian pines. Microb Ecol 76:839–850

Sperschneider J, Dodds PN, Gardiner DM, Singh KB, Taylor JM (2018) Improved prediction of fungal effector proteins from secretomes with EffectorP 2.0. Mol Plant Pathol 19:2094–2110

Spjut R, Simon A, Guissard M, Magain N, Sérusiaux E (2020) The fruticose genera in the Ramalinaceae (Ascomycota, Lecanoromycetes): their diversity and evolutionary history. MycoKeys 73:1

Spjut R (1996) *Niebla* and *Vermilacinia* (Ramalinaceae) from California and Baja California. BRIT Press

Stanke M, Keller O, Gunduz I, Hayes A, Waack S, Morgenstern B (2006b) AUGUSTUS: ab initio prediction of alternative transcripts. Nucleic Acids Res 34:W435–W439

Stanke M, Tzvetkova A, Morgenstern B (2006) AUGUSTUS at EGASP: using EST, protein and genomic alignments for improved gene prediction in the human genome. Genome Biol 7(Suppl. 1):S11.11-S11.18

Stanton D, Horn H (2013) Epiphytes as "filter-drinkers": life-form changes across a fog gradient. Bryologist 116:34–42

Summerell BA (2019) Resolving *Fusarium*: Current status of the genus. Ann Rev Phytopathol 57:323–339

Syme RA, Martin A, Wyatt NA, Lawrence JA, Muria-Gonzalez MJ et al (2018) Transposable element genomic fissuring in *Pyrenophora teres* is associated with genome expansion and dynamics of host-pathogen genetic interactions. Front Genet 9:130

Sérusiaux E, Van den Boom P, Ertz D (2010) A two-gene phylogeny shows the lichen genus Niebla (Lecanorales) is endemic to the New World and does not occur in Macaronesia nor in the Mediterranean basin. Fungal Biol 114:528–537

Taole M, Bihon W, Wingfield BD, Wingfield MJ, Burgess TI (2015) Multiple introductions from multiple sources: invasion patterns for an important Eucalyptus leaf pathogen. Ecol Evol 5:4210–4220

Tavare S (1986) Some probabilistic and statistical problems in the analysis of DNA sequences. In: Muira RM (ed) Some mathematical questions in biology: DNA sequence analysis. The American Mathematical Society, Providence, RI

Ter-Hovhannisyan V, Lomsadze A, Chernoff YO, Borodovsky M (2008) Gene prediction in novel fungal genomes using an *ab initio* algorithm with unsupervised training. Genome Res 18:1979–1990

Turo C, Mair WJ, Martin,A, Ellwood SR, Oliver RP, et al (2020) Genetic recombination and clonality in *Pyrenophora teres* populations in Western Australia.

Vanderpool D, Bracewell RR, McCutcheon JP (2017) Know your farmer: ancient origins and multiple independent domestications of ambrosia beetle fungal cultivars. Mol Ecol 27:2077–2094

Vaser R, Sovic I, Nagarajan N, Sikic M (2017a) Fast and accurate de novo genome assembly from long uncorrected reads. Genome Res 27:737–746

Vaser R, Sović I, Nagarajan N, Šikić M (2017b) Fast and accurate de novo genome assembly from long uncorrected reads. Genome Res 27:737–746

Walker B, Abeel T, Shea T, Priest M, Abouelliel A et al (2014) Pilon: an integrated tool for comprehensive microbial variant detection and genome assembly improvement. PLOS ONE 9:e112963

Walker BJ, Abeel T, Shea T, Priest M, Abouelliel A et al (2014) Pilon: an integrated tool for comprehensive microbial variant detection and genome assembly improvement. PLOS ONE 9(11):112963

Wang Y, Yuan X, Chen L, Wang X, Li C (2018) Draft genome sequence of the lichen-forming fungus *Ramalina intermedia* strain YAF0013. Genome Announc 6:e00478-18

Wiemann P, Sieber CMK, Von Bargen KW, Studt L, Niehaus E-M et al (2013) Unleashing the cryptic genome: genome-wide analyses of the rice pathogen *Fusarium fujikuroi* reveal complex regulation of secondary metabolism and novel metabolites. PLoS Pathogens 9:e1003475

Wikler K, Gordon TR (2000) An initial assessment of genetic relationships among populations of *Fusarium circinatum* in different parts of the world. Can J Bot 78:709–717

Wilken PM, Aylward J, Chand R, Grewe F, Lane FA et al (2020) IMA Genome - F13: Draft genome sequences of *Ambrosiella cleistominuta, Cercospora brassicicola, C. citrullina, Physcia stellaris*, and *Teratosphaeria pseudoeucalypti*. IMA Fungus 11:19

Wingfield BD, Barnes I, De Beer ZW, De Vos L, Duong TA et al (2015) Draft genome sequences of *Ceratocystis eucalypticola, Chrysoporthe cubensis, C. deuterocubensis, Davidsoniella virescens, Fusarium temperatum, Graphilbum fragrans, Penicillium nordicum,* and *Thielaviopsis musarum*. IMA Fungus 6:493–506

Wingfield MJ, Crous PW, Boden D (1996) *Kirramyces destructans* sp. nov., a serious leaf pathogen of Eucalyptus in Indonesia. SAJ Bot 62:325–327

Wingfield BD, Fourie A, Simpson MC, Bushula-Njah VS, Aylward J et al (2019) IMA Genome-F 11 Draft genome sequences of *Fusarium xylarioides, Teratosphaeria gauchensis* and *T. zuluensis* and genome annotation for *Ceratocystis fimbriata*. IMA Fungus 10:13

Wingfield BD, Liu M, Nguyen HD, Lane FA, Morgan SW et al (2018) Nine draft genome sequences of *Claviceps purpurea s. lat., including C. arundinis, C. humidiphila, and C. cf. spartinae,* pseudomolecules for the pitch canker pathogen *Fusarium circinatum,* draft genome of *Davidsoniella eucalypti, Grosmannia galeiformis, Quambalaria eucalypti,* and *Teratosphaeria destructans*. IMA Fungus 9:401–418

Duong *et al. IMA Fungus* (2021) 12:30

Page 17 of 17

Wingfield BD, Steenkamp ET, Santana QC, Coetzee MPA, Bam S et al (2012) First fungal genome sequence from Africa: a preliminary analysis. SAJ Sci 108:1–9

Wingfield BD, Van Wyk M, Roos H, Wingfield MJ (2013) *Ceratocystis*: emerging evidence for discrete generic boundaries. In: Seifert KA, De Beer ZW, Wingfield MJ (eds) The Ophiostomatoid Fungi: Expanding Frontiers, vol 12. CBS-KNAW Fungal Biodiversity Centre CBS, Utrecht, pp 57-64

Wyatt NA, Richards JK, Brueggeman RS, Friesen TL (2020) A Comparative Genomic Analysis of the Barley Pathogen *Pyrenophora teres f. teres* Identifies Subtelomeric Regions as Drivers of Virulence. Mol Plant-Microbe Interact 33:173–188

Yilmaz N, Sandoval-Denis M, Lombard L, Visagie CM, Wingfield BD et al (2021) Redefining species limits in the *Fusarium fujikuroi* species complex. Persoonia 46:129–162

Publisher's Note

Springer Nature remains neutral with regard to jurisdictional claims in published maps and institutional affiliations.